Molecular Analysis of Drug Delivery Systems Controlled by Dissolution of the Polymer Carrier

BALAJI NARASIMHAN AND NIKOLAOS A. PEPPAS[X]

Received September 4, 1996, from the *Biomaterials and Drug Delivery Laboratories, School of Chemical Engineering, Purdue University, West Lafayette, IN 47907-1283.* Final revised manuscript received October 23, 1996. Accepted for publication November 19, 1996[⊗].

Abstract □ Dissolution-controlled drug delivery systems are characterized by a phase erosion of the polymer carrier that is associated with fast or slow dissolution of the macromolecular chains. The molecular nature of the dissolution phenomenon was examined by analyzing the water transport process and the subsequent polymer chain disentanglement that is usually characterized by a snake-like motion of the chain (reptation). The results indicate that the polymer molecular weight, water, polymer and drug diffusion coefficients, equilibrium water concentration in the polymer, and water-polymer interaction parameter can control the mechanism and rate of drug release. A new model for this process was developed, and its predictions are compared with experimental studies of drug delivery from poly(vinyl alcohol)-based systems.

A number of swelling-controlled release systems for the delivery of drugs, peptides, or proteins function by a process of continuous swelling of the polymer carrier that is associated with simultaneous or subsequent dissolution of the polymer carrier.[1−3] As such, these dissolution-controlled release systems (where dissolution of the polymer carrier controls the drug release) have similar characteristics to many biodegradable systems. As Lee[4] pointed out in his pioneering work in 1980, phase erosion-based systems include those in which the polymer carrier is eliminated either by degradation or by dissolution, thus allowing the incorporated drug to be released in the surrounding medium.

Swelling-controlled release systems consist of a drug molecularly dispersed or dissolved in a polymer matrix at low or high concentrations. As water penetrates the polymer, swelling occurs and a thin layer of polymer in the rubbery state (gel layer) is formed. Drug diffusion through this gel layer is relatively fast. Previous studies[5−7] have shown that drug delivery from such systems is governed by the gel layer thickness. During drug delivery, as swelling and dissolution compete,[8−12] the gel layer thickness first increases due to swelling (region a of Figure 1), then remains constant due to synchronization of swelling, drug diffusion, and dissolution (region b, Figure 1), and finally decreases as dissolution takes over (region c, Figure 1; note that the gel layer thickness in Figure 1 has been normalized with respect to the initial half thickness of the polymer).

The process of drug release from swelling-controlled release systems that exhibit dissolution has been described by relatively simple steps and expressions[13,14] that do not describe well the molecular phenomena involved. The model of Lee and Peppas[13] predicts that the gel layer thickness is directly proportional to the square root of release time, whereas the model of Harland et al.[14] uses a mass transfer coefficient to control the dissolution. However, recently there has been significant new work and understanding of the molecular interpretation of polymer dissolution.[11,15] Thus, it has become possible to better analyze drug release from dissolution-controlled systems. Our work provides an exact molecular interpretation of the phenomena along with a new model for drug release prediction.

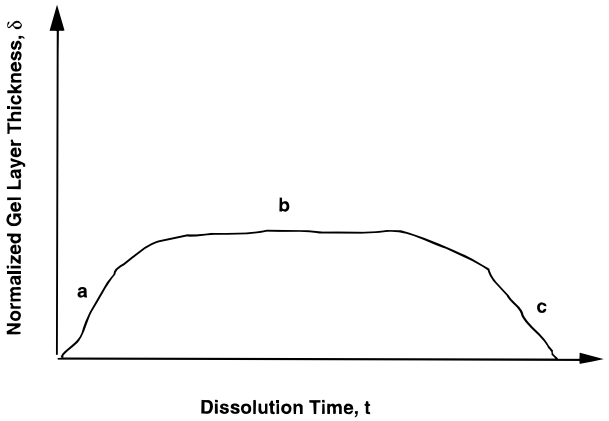

Figure 1—Dependence of normalized gel layer thickness, δ, on the dissolution time, t, for dissolving polymer systems in the absence or presence of drugs.

Theoretical Section

Physical Description and Model Development—We consider a thin swellable, hydrophilic glassy polymer film (or slab or disk) loaded with a water soluble, crystalline drug at a concentration, $v_{d,0}$. The ensuing drug delivery system is placed in contact with water or a biological fluid. During the first stage of the release process, the glassy polymer of initial thickness $2l$ (Figure 2a) starts swelling due to water penetration and the simultaneous transition from the glassy to the rubbery state. Thus, as shown in Figure 2b, two distinct fronts are observed, the swelling interface at position R and the polymer−water interface at position S. Initially, front R moves inwards whereas front S moves outwards as long as swelling prevails. When the concentration of the penetrant (water) in the polymer exceeds a critical value, v_1*, macromolecular disentanglement begins (as indicated in Figure 2c) and both R and S diminish. This critical concentration, v_1*, is the concentration at which true polymer dissolution commences. After macromolecular disentanglement is complete, the polymer is dissolved. Obviously, during the latter part of the dissolution period, both fronts R and S move towards the center of the slab. After the disappearance of the glassy core, only front S exists and it continues to move inwards towards the center of the slab until all of the polymer is dissolved (Figure 2d). The positions of the fronts can be readily followed experimentally with optical or polarized microscopy as previously reported by us[10] and others.[16,17]

The macromolecular disentanglement mechanism is shown in Figure 3, where the disentanglement of the "bold" chain is considered. A test chain in an entangled system of chains is shown in Figure 3a. When solvent penetrates into this system, the mobility of the test chain increases, and the chain begins to exhibit "reptation". It has been shown by De

[⊗] Abstract published in *Advance ACS Abstracts,* January 15, 1997.

S0022-3549(96)00372-3 CCC: $14.00

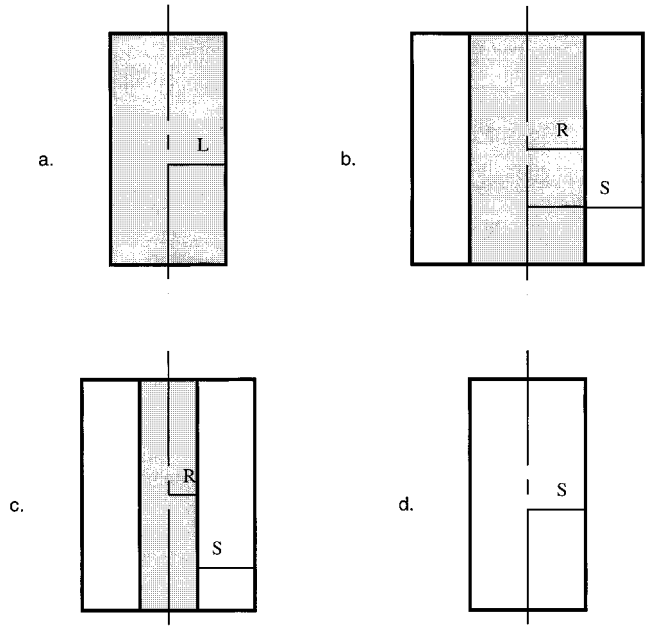

Figure 2—Schematic representation of a one-dimensional solvent diffusion and polymer dissolution process: (a) initial slab thickness, 2*l*; (b) initial swelling step showing the increasing position of the rubbery/solvent interface, S, and the decreasing position of the glassy/rubbery interface, R; (c) beginning of the dissolution step showing the decreasing position of the interface S along with the decreasing position of the interface R; and (d) final dissolution step where the slab has been transformed into a rubbery material (disappearance of interface R) and the position of interface S still decreases.

Gennes[23,24] that the snake-like motion of a polymer chain (termed "reptation") dominates transport in an entangled system. The time taken for the front end of the chain to reach the point where the rear end of the chain has been at $t = 0$ is called reptation time. Reptation causes the test chain to disentangle from the system (Figure 3b). The test chain completely disentangled from the original system is shown in Figure 3c.

During the dissolution process, the polymer carrier passes through three distinct regimes of macromolecular configuration, as indicated in Figure 4. Clearly, the diffusional behavior of the drug is affected by the state of these regimes, as the drug diffusion coefficient is a function of polymer concentration. Thus, the swollen rubbery layer is the concentrated regime, indicated in Figure 4a, where the chains are completely entangled. The semidilute regime (Figure 4b) is a diffusion boundary layer just outside the rubber/solvent interface S in the solvent. In the boundary layer, the chains are just disentangling. When the polymer is fully dissolved, the completely disentangled chains move freely in the solvent and exhibit Brownian motion; this is the dilute regime indicated in Figure 4c. Having characterized the entire concentration range into these regimes, our approach is to write water and drug transport equations in each of these regimes and couple them through conditions at the moving boundary.

We have developed a one-dimensional water and drug diffusion followed by chain disentanglement in amorphous, uncrosslinked, linear polymers. This model describes transport in a film, slab, disk, or tablet in the x direction. The assumption of one-dimensional transport may be relaxed without loss of generality. A three-component system is considered, with the water indicated as component 1, the polymer as component 2, and the drug as component d.

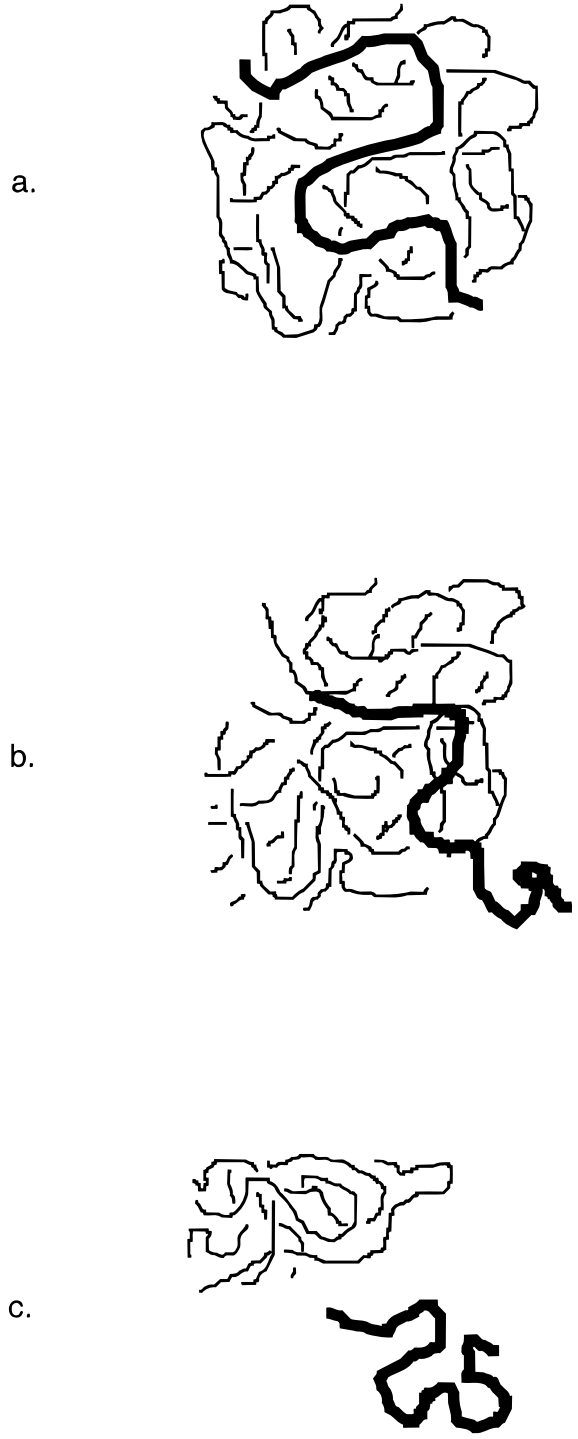

Figure 3—Macromolecular disentanglement indicating the successive processes of (a) a system of entanged chains, (b) a reptating chain "disentangling" from the system, and (c) a completely disentangled chain.

Water transport may be expressed by a generalized Fick's law as follows:

$$\frac{\partial v_1}{\partial t} = \frac{\partial}{\partial x}\left(D_1 \frac{\partial v_1}{\partial x}\right) \tag{1}$$

In eq 1, v_1 is the volume fraction of water in the swollen polymer and D_1 is the water diffusion coefficient in the polymer. Equation 1 is valid in the slab region between $x =$ R and $x =$ S (see Figures 2b and 2c). Drug transport and

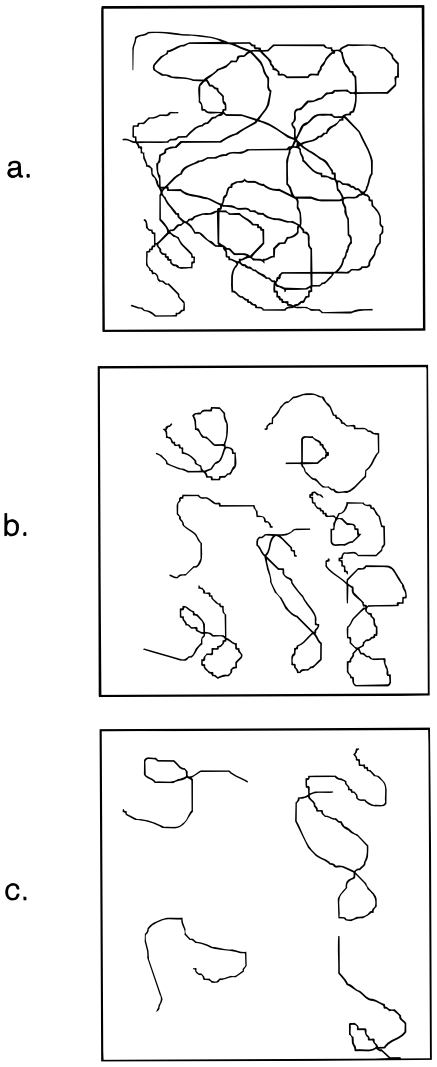

Figure 4—The solvent concentration field varies during polymer dissolution in a controlled-release device. (a) Before dissolution starts, there is no disentanglement in a swellable system (concentrated regime. (b) The onset of dissolution in the diffusion boundary layer leads to the semi-dilute regime. (c) Finally, the dissolution is complete and the disentangled chains exhibit Brownian motion in the solvent in the dilute regime.

release out of the polymer is also described by a generalized Fick's law as follows:

$$\frac{\partial v_d}{\partial t} = \frac{\partial}{\partial x}\left(D_d \frac{\partial v_d}{\partial x}\right) \tag{2}$$

In eq 2, v_d is the volume fraction of drug in the polymer and D_d is the drug diffusion coefficient in the polymer.

Equations 1 and 2 describe the overall swelling/dissolution/release process and can be solved with the following initial conditions:

$$t = 0 \qquad \forall\ x \qquad v_1 = 0 \tag{3a}$$

$$t = 0 \qquad \forall\ x \qquad v_d = v_{d,0} \tag{3b}$$

The moving boundary condition at the glassy–rubbery interface is given by a mass balance at the interface R:

$$(v_1 + v_d)\frac{dR}{dt} = -\left(D_1 \frac{\partial v_1}{\partial x}\right) - \left(D_d \frac{\partial v_d}{\partial x}\right) \tag{4}$$

Table 1—Linear Expansion Coefficients of Selected Polymers Used as Carriers in Drug Delivery[a]

Polymer	Linear Expansion Coefficient, $\alpha_f \times 10^4$ (K^{-1})
Cellulose	0.075
Polybutadiene	7.5
Poly(dimethyl siloxane)	10.9
Polyethylene	1.1
Poly(ethylene terephthalate)	2.2
Poly(2-hydroxyethyl methacrylate)	3.7
Poly(methyl acrylate)	4.0
Poly(methyl methacrylate)	3.2
Polypropylene	0.4
Polystyrene	3.7
Poly(vinyl acetate)	4.4
Poly(vinyl alcohol)	3.7
Poly(vinyl chloride)	1.1

[a] According to Ferry,[18] the linear expansion coefficient, α_f, is equivalent to $\Delta\alpha$, where $\Delta\alpha = \alpha_l - \alpha_g$; here, α_l is the expansion coefficient above T_g and α_g is the expansion coefficient below T_g.

The initial condition for eq 4 is that at $t = 0$, R = l, which is the half thickness of the polymer slab. The water and drug volume fractions at the interface R, v_1* and v_d*, respectively, are functions of the thermodynamic conditions of the glassy–rubbery transition. These values are given as follows:

$$t > 0 \qquad x = R \qquad v_1 = v_1^* \tag{5a}$$

$$t > 0 \qquad x = R \qquad v^d = v_d^* \tag{5b}$$

These two volume fractions can be determined by unique expressions based on the free volume theory, as expressed by eqs 6a and 6b:

$$v_2^* = \frac{\frac{1}{\rho_2}}{\frac{1}{\rho_2} + \frac{(T_g - T)}{(\beta/\alpha_f)}\cdot\frac{1}{\rho_1} + \frac{1}{\rho_d}} \tag{6a}$$

and

$$v_d^* = \frac{\frac{1}{\rho_d}}{\frac{1}{\rho_2} + \frac{(T_g - T)}{(\beta/\alpha_f)}\cdot\frac{1}{\rho_1} + \frac{1}{\rho_d}} \tag{6b}$$

Here, T_g is the glass transition temperature, T is the experimental temperature, α_f is the linear expansion coefficient of the polymer,[18,19] β is the expansion coefficient contribution of the water to the polymer,[19,20] ρ_1 is the water density, ρ_2 is the polymer density, and ρ_d is the drug density. Ferry[18] provided the relevant parameters for many polymer–solvent systems.

In this work, we have gathered or calculated relevant information from various sources on the properties of polymers, especially those relevant to pharmaceutical applications. The values of α_f and β for various polymer-solvent systems are presented in Tables 1 and 2. According to Ferry,[18] the linear expansion coefficient, α_f, is equivalent to $\Delta\alpha$, where $\Delta\alpha = \alpha_l - \alpha_g$. (Here, α_l is the expansion coefficient above T_g and α_g is the expansion coefficient below T_g.) The β values presented in Table 2 were calculated by the method suggested by Fujita and Kishimoto.[20] It must be noted that Ferry's original equations[18] were expressed in mass fractions, and we have conveniently translated the mass fractions into volume fractions in the form of eqs 6a and 6b. The use of volume

Table 2—Expansion Coefficient Contribution, β, of Water to Polymer Expansion in Systems Used in Drug Delivery[a]

Polymer	Expansion Coefficient, β
Cellulose I	0.20
Polybutadiene	0.20
Poly(dimethyl siloxane)	0.20
Polyethylene	0.20
Poly(2-hydroxyethyl methacrylate)	0.20
Poly(methyl acrylate)	0.30
Poly(methyl methacrylate)	0.15
Polypropylene	0.20
Polystyrene	0.14
Poly(vinyl acetate)	0.37
Poly(vinyl alcohol)	0.20
Poly(vinyl chloride)	0.20

[a] All values were determined by the Fujita-Kishimoto[20] method.

Table 3—Polymer-Water Parameters of Selected Polymer Carriers Used in Drug Delivery Systems[a]

Polymer	Polymer Density, ρ_2 (g/cm^3)	Polymer Glass Transition Temperature, T_g (°C)	Critical Polymer Volume Fraction, v_2*
Carboxymethylcellulose, Na salt	1.626	78	0.89
Hydroxyethyl Cellulose	1.378	106	0.85
Hydroxypropyl cellulose	1.094	124	0.85
Hydroxypropyl methylcellulose	1.366	155	0.77
Methylcellulose	1.386	196	0.71
Poly(2-hydroxyethyl methacrylate)	0.852	55	0.97
Poly(vinyl alcohol)	1.269	85	0.89

[a] All calculations were done with eq 6b, with a water density of $\rho_1 = 0.998$ g/cm^3 and a drug density of $\rho_d = 1.4$ g/cm^3 at 37 °C.

fractions is preferred here because of the moving boundary nature of the dissolution problem studied. Thus, based on these equations, we calculate the values of T_g and v_2* (with eq 6a) at 37 °C for various polymer−solvent systems (see Table 3).

The value of v_2* increases with increase in the hydrophilicity of the polymer (Table 3). Thus, in the case of hydroxypropyl methylcellulose, when 23% by volume of water penetrates into the polymer, it is transformed into a gel, whereas for poly(vinyl alcohol), 11% of water is sufficient to transform the polymer into a gel. Also, polymers with lower T_g values yield higher values of v_2*. It is worthwhile mentioning that eq 6a can only be used for compatible polymer-solvent systems ($\chi < 0.5$, where χ is the Flory polymer-solvent interaction parameter). Using eq 6a for noncompatible systems (for instance, polystyrene-water) will yield absurd values for v_2*. Another consideration is that the systems in Table 3 all involve water, although buffers and biological fluids are used as penetrants in some pharmaceutical applications. It is expected that the v_2* values in such systems would be lower because of interactions such as partitioning and hydrogen bonding in the system.

In addition to eqs 5a and 5b, an additional boundary condition is needed in the polymer. However, it must be noted that the boundary condition expressing the symmetry condition usually written during penetrant or drug diffusion into polymers is not valid here as long as the glassy core is present. If invoked, it will lead to erroneous results like in the case of the model of Ju et al.,[21] where this condition was regretfully applied in the glassy layer as well. The symmetry boundary condition of eq 7 is valid only when the sample has become one continuous phase, as for example when the polymer becomes purely rubbery in our case (i.e., when the front R disppears):

$$t > 0 \qquad x = 0 \qquad \mathrm{R} = 0 \qquad \frac{\partial v_1}{\partial x} = 0 \tag{7}$$

Finally, the water and drug volume fractions, $v_{1,eq}$ and $v_{d,eq}$, respectively, at the rubbery−solvent interface S are given as follows:

$$t > 0 \qquad x = \mathrm{S} \qquad v_1 = v_{1,eq} \tag{8a}$$

$$t > 0 \qquad x = \mathrm{S} \qquad v_d = \partial_{d,eq} \tag{8b}$$

The equilibrium water volume fraction, $v_{1,eq}$, can be estimated with the Flory-Rehner equation[22] for the swollen temporary network formed by the system entanglements. The first three terms in eq 9 arise out of the thermodynamic assumption that the chemical potential of the solvent in the polymer is equal to that just outside the polymer. The fourth term accounts for the elastic force that exists due to the presence of entanglements in the system.

$$\ln v_{1,eq} + \left(1 - \frac{1}{x}\right)(1 - v_{1,eq}) + \chi (1 - v_{1,eq})^2 + \bar{V}_1 \rho_2 \left(\frac{2}{\bar{M}_c} - \frac{1}{\bar{M}_n}\right)\left[\frac{2}{1 - v_{1,eq}} - (1 - v_{1,eq})\right] = 0 \tag{9}$$

In eq 9, x is the ratio between the molar volumes of the polymer and the water, χ is the polymer−water interaction parameter, $\bar{V}_1$ is the molar volume of water, $\bar{M}_c$ is the critical molecular weight of the polymer, and $\bar{M}_n$ is the number average molecular weight of the polymer. The term x is defined as follows:

$$x = \frac{\bar{M}_n \bar{v}}{\bar{V}_1} \tag{10}$$

where $\bar{v}$ is the specific volume of the polymer and $\bar{V}_1$ is the molar volume of the solvent.

Similarly, the equilibrium drug volume fraction, $v_{d,eq}$, can be estimated with a modified Flory-Rehner equation for the temporary network. In this case, the term due to the entanglements appears as the drug diffusion is a function of the entanglement density of the polymer. The equilibrium drug volume fraction, $v_{d,eq}$, is calculated as follows:

$$\ln v_{d,eq} + \left(1 - \frac{1}{x_d}\right)(1 - v_{d,eq}) + \chi_d (1 - v_{d,eq})^2 + \bar{V}_d \rho_2 \left(\frac{2}{\bar{M}_c} - \frac{1}{\bar{M}_n}\right)\left[\frac{2}{1 - v_{d,eq}} - (1 - v_{d,eq})\right] = 0 \tag{11}$$

In eq 11, x_d is the ratio between the molar volumes of the polymer and the drug and χ_d is the polymer−drug interaction parameter. Similar to eq 10, x_d is given by:

$$x_d = \frac{\bar{M}_n \bar{v}}{\bar{V}_d} \tag{12}$$

In eq 12, $\bar{V}_d$ is the molar volume of the drug. The set of equations just presented completes the formulation of a model for the swelling/release process.

For description of drug transport, we assume that as the polymer chains disentangle, they move out of the gel-like state through a diffusion boundary layer (semi-dilute regime) of thickness δ_b. The polymer chain transport through this boundary layer is described as follows:

$$\frac{\partial v_2}{\partial t} = \frac{\partial}{\partial x}\left(D_p \frac{\partial v_2}{\partial x}\right) - \frac{dS}{dt}\frac{\partial v_d}{\partial x} \quad (13)$$

In eq 13, the second term in the right hand side of the equation indicates the moving boundary nature of the problem. Equation 13 is valid in the diffusion boundary layer of constant thickness δ_b.

The initial condition for the solution of eq 13 is as follows:

$$t = 0 \qquad \forall\, x \qquad v_2 = 0 \quad (14)$$

At the exterior of the boundary layer, the conventional boundary condition can be written as follows:

$$t > 0 \qquad x = S(t) + \delta_b \qquad v_2 = 0 \quad (15)$$

The boundary condition on the water side of the gel−solvent interface can be written by considering that a polymer chain requires a minimum time to disentangle and move out of the gel. The minimum time taken by the chains to disentangle has been defined as the reptation time (t_{rept}). Hence, the disentanglement rate is zero at the beginning of the release process and until a time equal to t_{rept}:

$$0 < t < t_{rept} \qquad x = S^+(t) \qquad -D_p \frac{\partial v_2}{\partial x} = 0 \quad (16)$$

After t_{rept}, chain transport at the gel−solvent interface may be either disentanglement-limited or diffusion-limited. At times just greater than t_{rept}, the rate of diffusion is sufficiently high and hence the flux is disentanglement-limited. Hence, the boundary condition can be written as follows:

$$t > t_{rept} \qquad x = S^+(t) \qquad -D_p \frac{\partial v_2}{\partial x} = k_d \quad (17)$$

where k_d is the chain disentanglement rate. The disentanglement rate can be calculated with the analysis given by Narasimhan and Peppas[11] as follows:

$$k_d = \frac{r_g}{t_{rept}} \quad (18)$$

where r_g is the radius of gyration of the polymer chains. The parameter r_g can be calculated by light scattering[25] experiments, whereas t_{rept} can be obtained from rheological experiments.[26]

As the chain disentanglement continues, polymer chains transfer to the water, and the polymer concentration in the boundary layer (semi-dilute regime, Figure 3b) increases until it reaches an equilibrium value, $v_{2,eq}$. At this point, the polymer diffusion rate becomes insufficient to transport the chains and hence the polymer concentration is always maintained at $v_{2,eq}$. Thus, an equilibrium exists between the polymer-rich gel state (concentrated regime) and the polymer-lean solution in the diffusion boundary layer (semi-dilute regime). Hence, the boundary condition becomes:

$$t > t_{rept} \qquad x = S^+(t) \qquad v_2^+ = v_{2,eq} \quad (19)$$

The water−rubbery state interface S moves due to polymer swelling and subsequent chain disentanglement. This movement can be expressed as follows:

$$\frac{dS}{dt} = \frac{D_1 v_{1,eq}}{v_{1,eq} + v_{d,eq}}\frac{\partial v_1}{\partial x} + \frac{D_d v_{d,eq}}{v_{1,eq} + v_{d,eq}}\frac{\partial v_d}{\partial x} - \frac{D_p}{v_{1,eq} + v_{d,eq}}\frac{\partial v_2}{\partial x} \quad (20)$$

The first term on the right-hand side of eq 20 describes the swelling of the polymer due to water penetration and the second term also describes swelling due to drug diffusion. The third term of the right-hand side describes the chain disentanglement mechanism. The initail condition for eq 20 is that at $t = 0$, $S = l$, the initial half thickness of the polymer slab.

Equations 1 through 20 complete the formulation of the moving boundary problem.

Experimental Section

Materials—A number of dissolution-controlled release systems can be analyzed with these models. Some of the systems were prepared as described by Harland et al.[14] Sodium diclofenac (Pharmatec, Milan, Italy; MW = 282.68; mp = 283−285 °C) was used as a model drug because of its good solubility in water and buffered solutions. The polymer carrier used was poly(vinyl alcohol) (PVA; Mowiol 40−88, Hoechst, Frankfurt, Germany; $\bar{M}_n$ = 130 000; degree of hydrolysis, 87.7%). Mannitol was used as a filler (Gianni, Milan, Italy; MW = 182.17; mp = 166−168 °C).

System Preparation—A mixture of 50 weight percent (wt %) sodium diclofenac, 20 wt % PVA, and 30 wt % mannitol was prepared and compressed as described by Colombo et al.[6] The tablets were coated on three sides with a 15 wt % acetone solution of cellulose acetate propionate (CAP; Eastman Kodak, Kingsport, TN). The coating was insoluble in and impermeable to the buffered solutions used, thus allowing for analysis of one-dimensional diclofenac release.

Polymer Dissolution and Drug Release Experiments—Polymer dissolution experiments were performed in 1-L USP dissolution cells at 37 °C. Diclofenac release studies were carried out in the same cells by analyzing the sodium diclofenac concentration at 275 nm with a UV spectrophotometer.

Results and Discussion

Steady-State Predictions—Solving the previously described dissolution/release problem results in a series of expressions that can be used for the analysis of various dissolution-controlled release systems. A mathematical solution at steady-state of the water, polymer, and drug transport model described by eqs 1 through 20 can be readily obtained. Typically, such mathematical solutions are based on the approximation of linear profiles of water and drug concentration in the swollen polymer, which is given by eqs 21 and 22, respectively:

$$v_1 = \frac{v_1^* S - v_{1,eq} R}{S - R} - \frac{v_1^* - v_{1,eq}}{S - R}x \quad (21)$$

and

$$v_d = \frac{v_d^* S - v_{d,eq} R}{S - R} - \frac{v_d^* - v_{d,eq}}{S - R}x \quad (22)$$

where

$$v_1^* = 1 - v_2^* - v_d^* \quad (23)$$

The moving boundary conditions (eqs 4 and 20) are transformed on substituting the concentration profiles (eqs 21 and 22) as follows:

$$(v_1^* + v_d^*)\frac{dR}{dt} = -\frac{D_1}{S - R}[v_{1,eq} - v_1^*] - \frac{D_d}{S - R}[v_{d,eq} - v_d^*] \quad (24)$$

and

$$\frac{dS}{dt} = \frac{v_{1,eq}}{(v_{1,eq} + v_{d,eq})(S - R)} \frac{D_1}{}[v_{1,eq} - v_1^*] + \frac{v_{d,eq}}{(v_{1,eq} + v_{d,eq})(S - R)} \frac{D_d}{}[v_{d,eq} - v_d^*] - \frac{k_d}{(v_{1,eq} + v_{d,eq})} \quad (25)$$

A term encountered in eqs 21−25 is the gel layer thickness, $\delta = S - R$, which represents the portion of the polymer slab that is in the rubbery state during the swelling/dissolution process. Dividing both sides of eq 24 by $(v_1^* + v_d^*)$ and subtracting from eq 25 results in a differential equation for δ. Solving the resultant equation with the condition that at $t = 0$, $\delta = 0$, the dependence of δ on time can be calculated as follows:

$$-\delta - \alpha \ln\left(1 - \frac{\delta}{\alpha}\right) = B\,t \quad (26)$$

where α is defined as follows:

$$\alpha = \frac{A}{B} \quad (27)$$

In eqs 26 and 27, A and B are defined as follows:

$$A = D_1 (v_{1,eq} - v_1^*)\left[\frac{v_{1,eq}}{v_{1,eq} + v_{d,eq}} + \frac{1}{v_1^* + v_d^*}\right] + D_d (v_d - v_{d,eq})\left[\frac{v_{d,eq}}{v_{1,eq} + v_{d,eq}} + \frac{1}{v_1^* + v^*_d}\right] \quad (28)$$

$$B = \frac{k_d}{v_{1,eq} + v_{d,eq}} \quad (29)$$

By integrating the concentration profile of the drug, the following expression for the fraction of the drug released can be derived:

$$\frac{M_d}{M_{d,\infty}} = \frac{\sqrt{B}(v_{d,eq} + v_d^*)}{2\,l}(\sqrt{2\alpha t} + \sqrt{B}\,t) \quad (30)$$

This expression indicates that under quasi-steady-state conditions, the amount of drug released, M_d, normalized with respect to the drug released at infinite time, $M_{d,\infty}$, is dependent on time and the square root of time. The various parameters appearing in this equation include the water and drug volume fractions at equilibrium at the concentrated/semi-dilute regimes (quantities with subscript eq) and at the transition front (quantities with superscript *); the water and drug diffusion coefficients, D_1 and D_d; the disentanglement rate, k_d; and the initial slab thickness, $2l$. As discussed before, the equilibrium conditions can be calculated from the thermodynamics of the system (see eqs 9 and 10), the transition conditions from structural characteristics of the polymer and the drug (eqs 6a and 6b), and the disentanglement rate from a combination of light scattering techniques and rheological studies, whereas the two diffusion coefficients may be determined by pulsed gradient spin echo nuclear magnetic resonance (NMR) spectroscopy.[27]

To investigate the influence of various parameters on the drug release behavior, we simulated the normalized drug released with eq 30. We considered a simple case of a thin disk of thickness $2l = 1$ mm, containing a drug with $v_{d,eq} = 0.10$ and $v_d^* = 0.05$. We considered water interactions such that $v_{1,eq} = 0.85$ and $v_1^* = 0.15$. Using a typical value[28] of $D_1 = 1.5 \times 10^{-6}$ cm^2/s, we calculated the release behavior for different size drugs with values of D_d ranging from 1×10^{-5} to 1×10^{-9} cm^2/s. As expected, the amount of drug released was higher for higher drug diffusion coefficients (Figure 5). Also, as α approached zero, Case II behavior (linear release profile) was observed, and for higher values of α, the drug release was Fickian. Small values of α are indicative of small D_d values, which in turn means large size drugs. This instance of small α values could happen with protein delivery, where unfolding of the protein before release could be the rate-limiting step, leading to Case II behavior for certain values of the protein unfolding rate. For higher values of α, the drug diffusion coefficient is high, indicating small size drugs. Such drugs diffuse in a Fickian manner as indicated by the simulation.

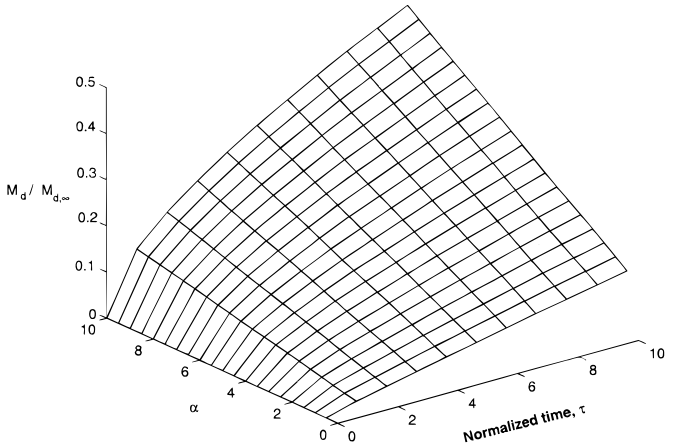

Figure 5—Predicted normalized drug released, $M_d/M_{d,\infty}$, as a function of normalized time, τ, for different values of α. The values of the parameters used in the simulation were $2l = 1$ mm $v_{d,eq} = 0.10$, $v_d^* = 0.05$, $v_{1,eq} = 0.85$, $v_1^* = 0.15$, $D_1 = 1.5 \times 10^{-6}$ cm^2/s, and $k_d = 2 \times 10^{-5}$ cm/s.

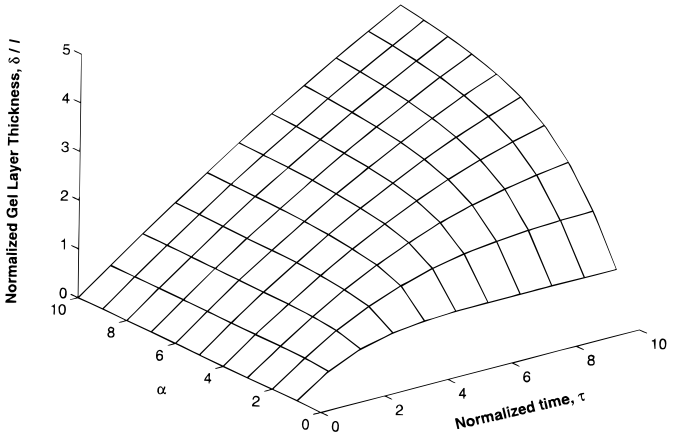

Figure 6—Predicted normalized gel layer thickness, δ/l, as a function of normalized time, τ, for different values of α. The values of the parameters are the same as in Figure 5.

In addition, we simulated the normalized gel layer thickness, δ, as a function of normalized time, τ, with eq 26. The normalized time, τ, is defined as follows:

$$\tau = \frac{B\,t}{l} \quad (31)$$

The values of the various parameters used were the same as in Figure 5. It is observed (Figure 6) that as α approaches zero, the gel layer thickness profile becomes flat (disentanglement-controlled), and for higher values of α, the gel layer thickness increases with time (diffusion-controlled). This observation is consistent with the trends shown by the normalized drug-release profile.

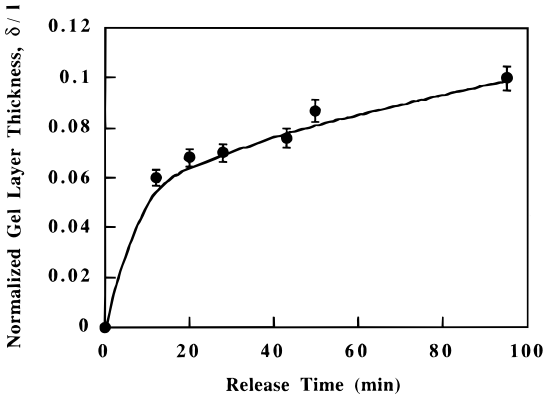

Figure 7—Normalized gel layer thickness versus time for dissolution of a tablet containing 50 wt % cimetidine hydrochloride, 10 wt % PVA ($\bar{M}_n$ = 130 000), and 40 wt % mannitol at 37 °C (data of Conte et al.[30]). The line represents the model predictions of eq 26.

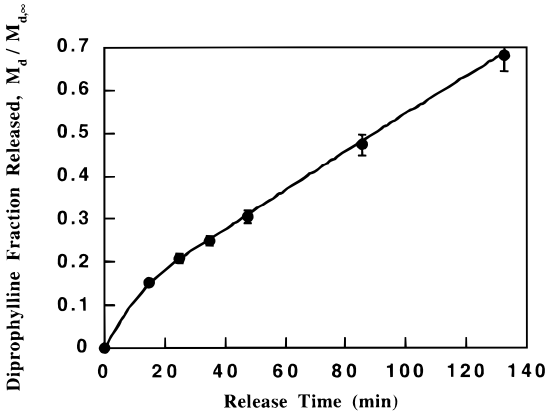

Figure 8—Normalized mass of diprophylline released versus time for dissolution of a tablet containing 50 wt % diprophylline, 10 wt % PVA ($\bar{M}_n$ = 130 000), and 40 wt % mannitol at 37 °C (data of Conte et al.[30]). The line represents the model predictions of eq 30.

Clearly, the fractional drug release dependence can be diffusion-controlled when the first term in the right-hand-side of eq 30 predominates. Indeed, this will lead to:

$$\frac{2A}{B^2} \gg 1 \qquad \frac{M_d}{M_{d,\infty}} = \sqrt{\frac{A}{2}\frac{(v_{d,eq} + v_d^*)}{l}}\sqrt{t} \tag{32}$$

Alternatively, the fractional drug release dependence can be disentanglement (dissolution)-controlled when the second term of the right-hand-side of eq 30 predominates; then, the following relationship exists:

$$\frac{2A}{B^2} \ll 1 \qquad \frac{M_d}{M_{d,\infty}} = \frac{k_d\,(v_{d,eq} + v_d^*)}{2l\,(v_{d,eq} + v_{1,eq})}t \tag{33}$$

Equation 33 indicates that the rate at which the drug is released in independent of time. Thus, by choosing solvent-polymer-drug systems such that $(2A/B^2) \ll 1$, zero-order drug-release systems can be obtained. The exact solution of the aforementioned problem is rather cumbersome and leads to a numerical algorithm that has been described elsewhere.[29]

Experimental Verification—Experimental verification of the quasi-steady-state analysis of the drug-release models was attempted with several systems. Three separate drug delivery systems were considered in this work, and the experimental results of drug release were compared with the model predictions. In addition, comparisons were made of the gel layer thickness as a function of time for those systems for which data were available.

Conte et al.[30] discussed the development and evaluation of controlled-release systems for the delivery of cimetidine hydrochloride. The system under consideration consisted of 50 wt% solution of cimetidine hydrochloride (MW = 288.79, $D_d = 1.3 \times 10^{-6}$ cm^2/s) formed in a tablet containing 30 wt% PVA of $\bar{M}_n$ = 130 000 and 20 wt% mannitol. Typical tablets tested had diameters of 10 mm and thicknesses of 2 mm. Drug dissolution was carried out in deionized water at 37 °C.

Data of the gel layer thickness, δ, of this system normalized with respect to the initial half thickness of the tablet, l, are plotted as a function of the release time in Figure 7. The same figure shows predictions of the gel layer thickness using eq 24. Here, D_1 was taken to be 1.5×10^{-5} cm^2/s for water transport in PVA, as reported by Tagikawa et al.,[31] and the equilibrium volume fractions of water and drug were calculated as $v_{1,eq} = 0.85$ and $v_{d,eq} = 0.10$ with eqs 9 and 10, respectively. The transition volume fractions of water and drug were calculated as $v_1^* = 0.15$ and $v_d^* = 0.05$ with eqs 6a and 6b respectively. The value of the disentanglement rate used was 2.0×10^{-5} cm/s according to Narasimhan and Peppas.[11] The model can give accurate predictions of the experimental data over a range of ~100 min. It must be noted that this is an independent prediction of the data and not a fitting.

Conte et al.[30] also studied the release of diprophylline (MW = 254, $D_d = 1.5 \times 10^{-6}$ cm^2/s) from a tablet containing 40 wt % drug, 40 wt % PVA of $\bar{M}_n$ = 130 000, and 20 wt % mannitol in deionized water. The tablet dimensions were the same as in the previous case and the experiments were carried out at 37 °C. The normalized fraction of drug released, $M_d/M_{d,\infty}$, as a function of time is shown in Figure 8. The predicted normalized amount of drug released as a function of time, determined with eq 30 is also shown in Figure 8. Again, the value of D_1 used was 1.5×10^{-5} cm^2/s according to Tagikawa et al.,[31] and the equilibrium volume fractions of water and drug were calculated as $v_{1,eq} = 0.85$ and $v_{d,eq} = 0.13$ with eqs 9 and 10, respectively. The transition volume fractions of water and drug were calculated as $v_1^* = 0.15$ and $v_d^* = 0.07$ with eqs 6a and 6b, respectively. The value of the disentanglement rate used was 2.0×10^{-5} cm/s according to Narasimhan and Peppas.[11] The agreement between the experimental data and the model predictions is very good.

Experimental results obtained in this work could also be predicted by this model. In the system studied, sodium diclofenac (MW = 318.13, $D_d = 1.1 \times 10^{-6}$ cm^2/s) was released from a system containing 30 wt% PVA of $\bar{M}_n$ = 130 000 and 20 wt % mannitol. The dissolution medium was intestinal stimulating fluid at 37 °C. The data for the normalized fraction of diclofenac released, $M_d/M_{d,\infty}$, as a function of time is presented in Figure 9. The normalized fraction of diclofenac was also predicted with eq 27, and this is also shown in Figure 9. Here, D_1 was assumed to be 1.1×10^{-5} cm^2/s, and the equilibrium volume fractions of intestinal fluid and drug were calculated as $v_{1,eq} = 0.76$ and $v_{d,eq} = 0.11$ with eqs 9 and 10, respectively. The transition volume fractions of intestinal fluid and drug were calculated as $v_1^* = 0.11$ and $v_d^* = 0.04$ with eqs 6a and 6b, respectively. As before, the value of the disentanglement rate used was 2.0×10^{-5} cm/s. Once again, the agreement is very good, thus verifying the validity of the model.

Clearly, the analyses reported herein indicate that polymer dissolution-controlled systems can be examined by the new model. The drug release behavior, as well as the slow change of the slab thickness with time, can be predicted. Thus, this model can be used for the design of novel dissolution-controlled systems. The parameters appearing in eqs 26 and 30 are readily determined for a given polymer/drug pair; therefore,

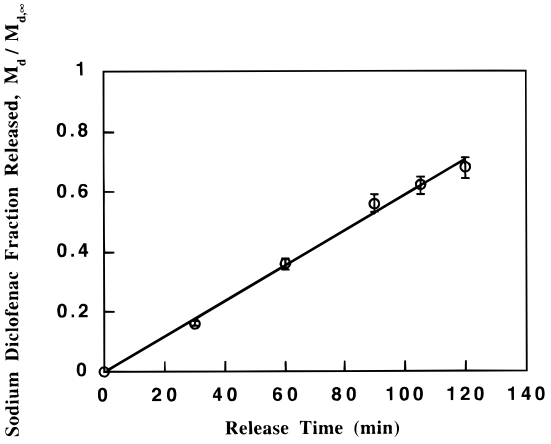

Figure 9—Normalized mass of sodium diclofenac released versus time for our studies of dissolution of a tablet containing 50 wt % sodium diclofenac, 30 wt % PVA ($\bar{M}_n$ = 130 000) and 20 wt % mannitol in intestinal simulating fluid at 37 °C. The line represents the model predictions of eq 30.

if necessary, systems can be designed that will exhibit zero-order release.

Conclusions

A new mathematical model was developed to describe the release of a drug from a dissolving polymer. Conditions for zero-order release were established. Approximate model solutions were verified with available experimental data and the agreement was good. This agreement suggested that suitable tuning of parameters that are related to the molecular properties of the water, the polymer, and the drug, such as the polymer molecular weight, the water and the drug diffusion coefficient, the equilibrium volume fractions of water and drug, and the water-polymer interaction parameter, could result in sustained zero-order release systems.

References and Notes

1. Korsmeyer, R. W.; Peppas, N. A. In *Hydrogels in Medicine and Pharmacy, Vol. III: Properties and Applications*; Peppas, N. A., Ed; CRC: Boca Raton, FL, 1987; pp 109−135.
2. Conte, U.; Maggi, L. *Biomaterials* **1996**, *17*, 889−896.
3. Narasimhan, B.; Peppas, N. A. *Adv. Polym. Sci.* **1997**, *128*, 157−207.
4. Lee, P. I. *J. Membr. Sci.* **1980**, *7*, 255−275.
5. Colombo, P.; Catellani, P. L.; Peppas, N. A.; Maggi, L.; Conte, U. *Int. J. Pharm.* **1992**, *88*, 99−109.
6. Colombo, P.; Gazzaniga, A.; Sangalli, M. E.; La Manna, A. *Acta Pharm. Technol.* **1987**, *33*, 15−20.
7. Colombo, P.; Bettini, R.; Massimo, G.; Catellani, P. L.; Santi, P.; Peppas, N. A. *J. Pharm. Sci.* **1995**, *8*, 991−997.
8. Parsonage, E. E.; Peppas, N. A.; Lee, P. I. *J. Vac. Sci. Technol.* **1987**, *B5*, 538−545.
9. Drummond, R. K.; Boydston, G. L.; Peppas, N. A. *J. Appl. Polym. Sci.* **1990**, *39*, 2267−2277.
10. Peppas, N. A.; Wu, J. C.; von Meerwall, E. D. *Macromolecules* **1994**, *27*, 5626−5638.
11. Narasimhan, B.; Peppas, N. A. *J. Polym. Sci., Polym. Phys.* **1996**, *34*, 947−961.
12. Mallapragada, S. K.; Peppas, N. A. *J. Polym. Sci., Polym. Phys.* **1996**, *34*, 1339−1346.
13. Lee, P. I.; Peppas, N. A. *J. Controlled Release* **1987**, *6*, 201−215.
14. Harland, R. S.; Gazzaniga, A.; Sangalli, M. E.; Colombo, P.; Peppas, N. A. *Pharm. Res.* **1988**, *5*, 488−494.
15. Narasimhan, B.; Peppas, N. A. *Macromolecules* **1996**, *29*, 3283−3291.
16. Papanu, J. S.; Hess, D. W.; Soane, D. S.; Bell, A. T. *J. Electrochem. Soc.* **1989**, *136*, 1195−1200.
17. Tu, Y. O.; Ouano, A. C. *IBM J. Res. Develop.* **1977**, *21*, 131−142.
18. Ferry, J. D. *Viscoelastic Properties of Polymers*, 3rd ed; John Wiley: New York, 1980.
19. Peppas, N. A.; Franson, N. M. *J. Polym. Sci., Polym. Phys.* **1983**, *21*, 983−997.
20. Fujita, H.; Kishimoto, A. *J. Polym. Sci.* **1958**, *28*, 547−567.
21. Ju, R. T. C.; Nixon, P. R.; Patel, M. V.; Tong, D. M. *J. Pharm. Sci.* **1995**, *84*, 1464−1477.
22. Flory, P. J.; Rehner, Jr., J. *J. Chem. Phys.* **1943**, *11*, 521−526.
23. De Gennes, P. G. *J. Chem. Phys.* **1971**, *55*, 571−579.
24. De Gennes, P. G. *Scaling Concepts in Polymer Physics*; Cornell University: Ithaca, NY, 1979.
25. Flory, P. J. *Principles of Polymer Chemistry*; Cornell University: Ithaca, NY, 1953.
26. Helfand, E.; Pearson, D. S. *J. Chem. Phys.* **1983**, *79*, 2054−2059.
27. von Meerwall, E. D. *Adv. Polym. Sci.* **1983**, *54*, 1−35.
28. Lustig, S. R.; Peppas, N. A. *J. Appl. Polym. Sci.* **1987**, *33*, 533−549.
29. Narasimhan, B.; Peppas, N. A., submitted to *Chem. Eng. Sci.*
30. Conte, U.; Colombo, P.; Gazzaniga, A.; Sangalli, M. E.; La Manna, A. *Biomaterials* **1988**, *9*, 489−493.
31. Takigawa, T.; Kasihara, H.; Masuda, T. *Polym. Bull.* **1990**, *24*, 613−618.

Acknowledgment

This work was supported by Grant no. CTS 92-12482 from the National Science Foundation.

JS960372Z